

Automation of the Fatigue Design Under Complex Loading

Jaime Tupiassú Pinho de Castro

Marco Antonio Meggiolaro

Mechanical Engineering Department

Pontifical Catholic University of Rio de Janeiro (PUC-Rio), Brazil

e-mails: jtcastro@mec.puc-rio.br, meggi@mit.edu

Copyright © 2000 Society of Automotive Engineers, Inc

ABSTRACT

A powerful software has been developed to automate *all* traditional local approach methods to calculate fatigue damage caused by complex loading: **SN**, **IW** (for welded structures) and **eN** to predict crack initiation, and **da/dN** for studying plane and 2D crack propagation, *considering* load sequence effects. This software runs on Windows environments and includes all necessary tools to perform the predictions, such as intuitive and friendly graphical interfaces in multiple idioms; several powerful databases for material properties, stress concentration factors, crack propagation rules, stress intensity factors, and the like; two (a traditional and a sequential) rain-flow counters and a load amplitude filter; graphical generators of *corrected* elastic-plastic hysteresis loops and of 2D cracks fronts; importing and automatic adjustment of experimental data; an equation interpreter; a complete help file, which includes an online advanced course on fatigue design; etc. Moreover, its damage models introduce various non-trivial innovations to improve the calculation speed and accuracy. In particular, a reliable and cost effective two-phase methodology is proposed to predict fatigue crack propagation in generic two-dimensional structural components under complex loading. First, the fatigue crack path and its stress intensity factor are calculated in a specialized finite-element companion software, using small crack increments. At each crack propagation step, the mesh is automatically redefined based on a self-adaptive strategy to calculate the crack propagation path and the stress-intensity factors **K_I**. Then, an analytical expression is adjusted to the calculated **K_I(a)** values, where **a** is the length along the crack path. Finally, this ex-

pression is used as an input to the da/dN module of the local approach software, where the complex loading is efficiently treated.

Key-words: Fatigue Design, Complex Loading, Automated Life Prediction.

INTRODUCTION

Fatigue is the type of mechanical failure characterized by the generation and/or gradual propagation of a crack, caused primarily by the repeated application of variable loads. These phenomena are progressive, cumulative and localized.

The crack generation usually starts from a notch, and depends primarily on the range of the *local* stress (**Ds**) or strain (**De**) acting on the critical or most loaded point of the structure. For design purposes, **Ds** and **De** should be calculated on a volume large in comparison to the microstructural parameter which characterizes the material anisotropy (e.g., the grain size in metals). When the cyclic loads are small (**Ds** macroscopically elastic), the phenomenon is much influenced by the local details of the material, surface finish, stress gradient, and residual stress state at the crack starting point. The resistance to fatigue crack initiation tends to increase with the ultimate strength **S_U**, the surface finish quality, the stress gradient, and the presence of compressive residual stresses at the critical point. These details are less important when the load is large, and cause macroscopic cyclic yielding at that point. In this case, the ductility is the main material fatigue strength controlling parameter.

Large cracks (larger than a few grain sizes) have their fatigue propagation rate (da/dN) controlled primarily by the mode I stress intensity range, ΔK_I . However, other parameters such as microstructure and mean loads are important when da/dN is either low (ΔK close to the propagation threshold ΔK_{th}) or high (K_{max} close to the material toughness K_C).

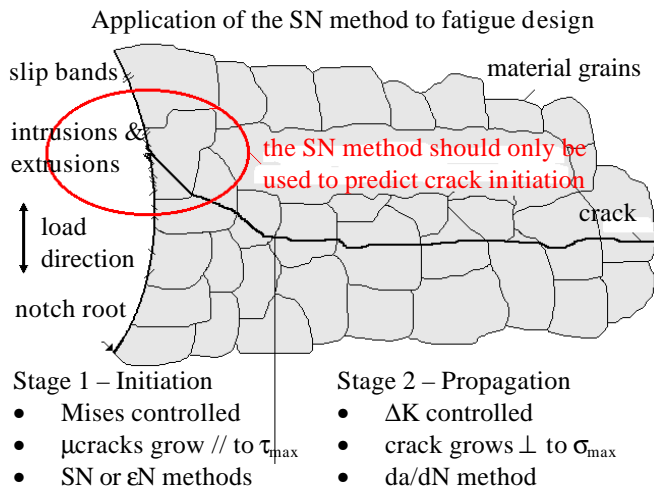


Figure 1 – The initiation and the propagation phases of the fatigue process.

The traditional methods to design against fatigue crack initiation are the SN and the ϵN . Welded structures are in general designed by a variation of the SN method, following the procedures of a welding institute such as the IIW or the AWS. The design against fatigue crack propagation follows the da/dN method, based on Fracture Mechanics concepts. All these methods are *local*, in the sense that their load history is completely described by the stress, strain or stress intensity acting on the critical point. In this manner, a strain gage and an appropriate stress concentration (K_t) or stress intensity (K_I) factor can provide all the loading information required to apply these design methods. In other words, *local* methods do not require the *global* solution of the stress and strain fields in the whole structure. This is physically sound, since fatigue damage is localized and normally does not spread to the rest of the structure.

All local design methods require information in six complementary areas of equal importance, namely:

- geometric dimensions (including notches and cracks, if present);
- service loads (that should preferably be measured, not estimated);
- material properties (that should also be measured);
- stress analysis (at the critical points, to predict crack initiation);
- crack analysis (to predict its propagation);
- damage accumulation (to deal with complex loads).

The accuracy of the predictions is controlled by the weakest link of this current, as illustrated in Figure 2.

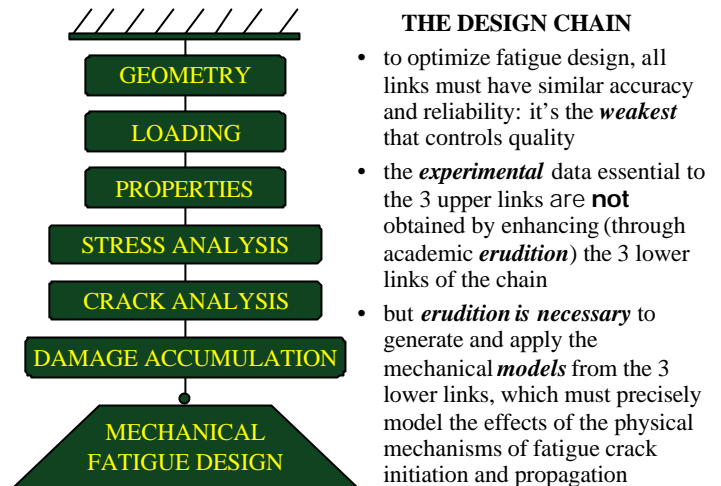


Figure 2 – The prediction accuracy is controlled by the weakest link of the fatigue design current

The sophistication of the stress, crack and damage analysis models (that depend on academic erudition) can not supply the experimental information required by the other links in practical applications. On the other hand, poor or incorrect calculation models simply can not generate appropriate predictions, even if reliable experimental data is available for the first three links. Besides, generous “safety” factors to correct the uncertainty of poor modeling can be economically unacceptable in competitive markets. In these cases, better models are indispensable for making reliable predictions, particularly when the loads are complex. But, the better the model, generally the greater the computational effort to apply it. That is why automation tools are becoming ever more important in real life applications, where the loads are usually complex.

Design automation tools must be precise, reliable, and as simple and fast to use as possible. Since there is no universal method to predict fatigue damage, they must be versatile too. In this way, besides the obvious requirements

1. to calculate fatigue damage by several design methods;
2. to include all the necessary sophistication to maximize the accuracy, the speed and the reliability of the calculations;
3. to allow for total control over the entire calculation process; and
4. to generate, export and print complete numerical and graphical reports;

a good software to automate the fatigue damage calculations must also

5. easily import, filter and count complex load data;
6. present a clear and intuitive graphical interface;
7. include all databases necessary to the design routines;
8. permit unlimited additions to the databases; and

- include all necessary documentation on the operational procedures and on the numerical and theoretical fundamentals of the calculation models.

The loads should be specified either in stress or in strain and their order must be preserved. The conversion between peak/valley and alternate/mean load sequences can be very useful. A rain-flow counter is a must, and an adjustable amplitude filter (to clean small load events that do not cause fatigue damage) can save a lot of time. To maintain most of the order information during the rain-flow counting, a sequential rain-flow algorithm can be advantageously used (this method counts the load events when they happen and not *before* their occurrence, as the traditional method does, see Figures 3a and 3b). Statistics are disarrayed, but load histograms should also be accepted, for use with fatigue models that do not recognize sequence effects. Probably the choice of a unit system is a plus, since designers are hard to change their (bad) habits. Finally, the automation software must plot the loads and also the counter and filter outputs, for visualization purposes.

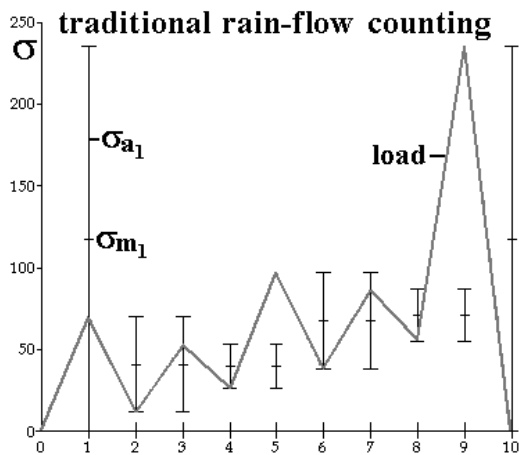


Figure 3a – Traditional rain-flow counting, anticipating the large load events.

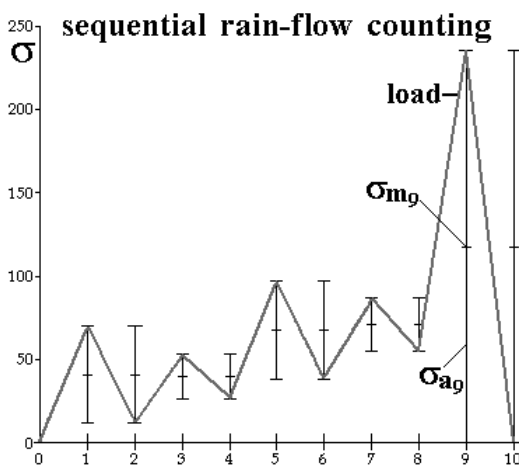


Figure 3b – Sequential rain-flow counting, which preserves most of the loading order.

The interface with the designer is extremely important. Nowadays, DOS-like commands are certainly out of the question. Intuitive graphical screens must be available for all calculation steps. The notation and the command buttons should have familiar appearance.

The databases must be as complete as possible. They must at least include material properties, stress concentration and intensity factors, crack propagation curves, and fatigue design data such as the effect of surface finish and notch sensitivity. All databases must be easily upgradable. Features to sort and to search the information by fields are a must. Database resources to estimate unavailable material properties or to parse analytical equations are very helpful when using or updating the stored information.

Finally, it is worth remembering that the fatigue failure phenomenology is quite complex. Many different mechanisms contribute to the crack initiation and propagation under alternating loads. It is no surprise there is no universal fatigue design method. Successful methodologies are at least partially empirical, and full of operational details. Therefore, no black-box calculation tool can be completely reliable, and automation software must be very well documented and completely controllable.

PRACTICAL IMPLEMENTATION OF AN AUTOMATION SOFTWARE

To automate the fatigue design routines by all these local methods, a powerful software named **V i d a** has been developed (*vida* means life in Portuguese, but it can also stand for Visual Damage calculator) [1]. It runs on Windows environments, has an intuitive and friendly graphical interface, is particularly useful to deal with complex loads considering sequence effects both in the initiation and in the propagation of one and two-dimensional (1D and 2D) fatigue cracks, and, among several others, includes all features discussed in this paper. Of particular academic interest are the innovations that had to be developed and implemented in the several fatigue design methods and computation routines to guarantee the reliability and to increase the speed of the calculations, such as:

- introduction of the ordered rain-flow counting method;
- the consideration of elastic-plastic overload effects on the SN method;
- a series of corrections in the traditional ϵN methodology, to guarantee the prediction of physically acceptable elastic-plastic hysteresis loops at a notch root;
- 1D and 2D crack propagation models with adjustable speed and precision, by the division of **DK** in two components, load and geometry, that can be updated at different rates;
- numerical filters to improve calculation efficiency;
- models to predict fatigue crack propagation and arrest after overloads;

- several extensive and resourceful databases;
- intuitive graphical format, using clear visual information and traditional notations, to eliminate any programming in the design process.

However, the automation of fatigue crack propagation life prediction under complex loading in intricate structural components is a still more challenging problem, that can not be solved by the local approach alone. But it can be divided into two complementary phases: first, the crack path and its associated stress intensity factor along the crack length \mathbf{a} , $\mathbf{K}_I(\mathbf{a})$, are calculated by *globally* modeling the structure using FE techniques, and second, this $\mathbf{K}_I(\mathbf{a})$ is used to *locally* calculate the crack growth, considering the loading complexities and retardation effects.

The global approach is almost indispensable to model the stress field in complex geometries, but its intense numerical calculation is not efficient when the load is complex. In the general case, fatigue loads cause different crack increments at each load cycle, requiring remeshing and time consuming recalculations in FE. Besides, crack retardation effects compromise even more the computational efficiency of the global approach.

On the other hand, the local approach, based on the direct integration of the crack propagation rule, can be efficiently used to calculate the crack increment at each load cycle, considering crack retardation effects if necessary. However, the integration of the crack propagation rule requires the stress intensity expression for the crack, which is simply not available for most real components. The error involved in using approximate \mathbf{K}_I handbook expressions to solve real problems obviously increases as the real crack path deviates from the tabulated one. Hence, in such cases the accuracy of the local approach is questionable and its predictions unreliable.

As the advantages of the two approaches are complementary, the FE calculated (under *simple* loading) $\mathbf{K}_I(\mathbf{a})$ along the crack length \mathbf{a} (following a path that is generally curved) can be used as an input to a local approach software, where the actual *complex* load can be efficiently treated by the direct integration of the crack propagation rule, considering retardation effects if required.

This hybrid methodology has been successfully implemented to study through-thickness cracks in arbitrary 2D structures, where the crack path is generally curved. If their path is known, such cracks can be described by *one* variable, the distance \mathbf{a} along their path, and in this sense behaving as 1D cracks. Therefore, they should not be confused with surface, corner or internal 2D cracks, which spread in 2D following an approximately elliptical front that can change its shape from cycle to cycle.

A specialized companion software called **QUEBRA2D** (*quebra* means break in Portuguese) is used to predict the curved crack path in complex 2D geometries, and to calculate its associated stress intensity factors. This software makes a finite element (FE) global discretization of the structure, using special purpose crack tip elements, self-adaptive mesh generation schemes and reliable crack increment criteria, as described elsewhere [2]. The various $\mathbf{K}_I(\mathbf{a})$, calculated under *simple* load at discrete crack increments, are adjusted by an appropriate analytical function. This function is then used in the **V i D a** software to predict the structure fatigue life under *complex* load, considering *any* da/dN crack propagation rule, and including retardation effects, if requested.

The fundamentals of the various methods to calculate fatigue damage caused by complex loading and their numerical implementation in these automation tools are briefly discussed below.

THE SN METHOD

The SN method correlates the number of cycles \mathbf{N} to initiate a fatigue crack in any structure with the life (in cycles) of small specimens that should (i) have the same fatigue strength (hence, the same material and details) and (ii) be submitted to the same stress history that loads the structure critical point (generally a notch root) in service.

The fatigue strength can be much influenced by the critical point details that can help or hinder the fatigue crack initiation and/or early propagation. The most important details are surface finish, stress gradient, micro residual stress and local material properties. Their effect is quantified by empirical strength modifiers factors, as discussed in any fatigue textbook [3-12]. It is recommended that these factors only be used for quantifying the effects of those details that act in a dimensional scale smaller than the parameter that characterizes the anisotropy of the material. Larger scale effects are better treated in the stress analysis. In addition, complex loads require the use of a damage accumulation model. Therefore, the SN design routine is:

- to evaluate the fatigue strength of the critical point,
- to calculate the stress history induced in the critical point by the real loading, and
- to quantify the accumulated fatigue damage caused by the various loading events.

As in the $\epsilon\mathbf{N}$ method, the SN method does not recognize the presence of cracks and, unlike the $\epsilon\mathbf{N}$, does not explicitly consider macroscopic plastic effects at the notch roots. Hence, the SN should only be applied to long initiation lives, when the stress histories are macroscopically elastic. However, the SN is simpler and computationally much faster than the $\epsilon\mathbf{N}$, counts with a vast database and a lot of accu-

mulated experience, and can be reliably used in many practical fatigue design cases.

The critical point fatigue strength is characterized by an SN (or Wöhler) curve and by a fatigue limit $S_L(N_L)$, if it exists (N_L is the number of cycles associated to S_L). The most used equation for the SN curve is parabolic

$$NS_f^B = C \quad (1)$$

and this form will be sustained in this work (however, the ideas developed below can easily be generalized for other forms of Wöhler curves). For calculation purposes, the fatigue strength information, including all above discussed effects, is contained in any three of the four numbers B , C , S_L , and N_L .

SN tests present a high dispersion, which generally increases with the fatigue life (lower lives are less dependent on randomly distributed local details to activate the cyclic dislocation movement responsible for the microcracks formation). Therefore, reliability concepts can be applied to SN curves and fatigue limits. SN curves can be plotted at 50% or at any other survival level. Higher reliability curves show up below the lower ones in an SN plane.

The load history can be measured (or estimated) at the critical or at a more conveniently located point (in this case the loads are called nominal). Since fatigue crack initiation involves microscopic dislocation movement even when the macroscopic stresses are elastic, it is the Tresca or the Mises component of the stress state acting at the critical point that must be used in the calculations.

The SN stress analysis is linear elastic, and obeys the superposition principle. Nominal stresses must be corrected to consider stress concentration effects at the critical point. However, due to their sharp stress gradients, small radius notches have a lower than K_t effect in long life fatigue. This effect is quantified by the fatigue stress concentration factor $K_f = 1 + q(K_t - 1)$, where q is the notch sensitivity factor. E.g., the stress analysis at a notch root (having bending K_{fM} and torsion K_{fT} fatigue stress concentration factors) in a circular shaft of diameter d , loaded by a force P which induces bending M and torsion T moments with alternate M_a and T_a and mean P_m and T_m components, would give the alternate and mean Mises stresses

$$s_{aMises} = \frac{16}{pd^3} \sqrt{(2K_{fM} M_a)^2 + 3(K_{fT} T_a)^2} \quad (2)$$

and

$$s_{mMises} = \frac{16}{pd^3} \sqrt{(2K_{fM} M_m)^2 + 3(K_{fT} T_m)^2} \quad (3)$$

The loading stress must be separated in alternate (s_a) and mean (s_m) components, as their effect is different in the fatigue process. Mean stress effects are quantified by an $s_a s_m$ rule, which should be understood as “the locus of the $s_a s_m$ combinations which cause the same fatigue damage on the point.” Several such rules (e.g. Goodman, Gerber or Soderberg) are used in fatigue design, but they are just a particular case of a more general elliptical rule

$$\frac{a}{c} \frac{s_a}{S_f(N)} \frac{0}{\theta}^{-r} + \frac{a s_m}{c S_m} \frac{0}{\theta}^{-s} = 1 \quad (4)$$

where $r = s = 1$ for Goodman and Soderberg, $r = 1$ and $s = 2$ for Gerber, $S_m = S_U$ for Goodman and Gerber and $S_m = S_Y$, the yield strength, for Soderberg. However, this elliptical rule should not be used for compressive mean loads, since they are beneficial to the fatigue strength. Therefore, it is suggested that a variation of the Goodman rule be used for $s_m < 0$:

$$\frac{s_a}{S_f(N)} + \frac{a s_m}{S_m} = 1 \quad (5)$$

where $a \geq 0$. If $a = 0$, the beneficial effect of the compressive mean load is ignored, and if $a = 1$ it is considered by a prolongation of the Goodman line in the compressive part of the $s_a s_m$ plane. Other values of a can be used to adjust reliable experimental data. If a non-linear fitting of the compressive mean load data is desired, the following adaptation of the elliptical rule

$$\frac{a}{c} \frac{s_a}{S_f(N)} \frac{0}{\theta}^{-rc} + \frac{a s_m}{|S_m|} \frac{a |S_m|}{c S_m} \frac{0}{\theta}^{-sc} = 1 \quad (6)$$

can be tried, but it is normally not used in fatigue design.

The treatment of complex loads, whose amplitude in general can randomly vary in time, requires a damage accumulation rule. Complex load events should be accounted for by the rain-flow (or by the sequential rain-flow) algorithm (which, by the way, count reversions or $1/2$ cycles). In the SN method, the damage caused by the i -th load event, which has (s_{a_i}, s_{m_i}) components acting during n_i cycles, is almost always defined by $d_i = n_i/N_i$, where N_i is the number of cycles that would cause fatigue failure if the load was simple with constant (s_{a_i}, s_{m_i}) components.

To calculate N_i , one should first calculate the alternated load $s_{a_{eqi}}$ that is equivalent (in the sense of causing the same fatigue damage) to (s_{a_i}, s_{m_i}) , according to Wöhler and a $s_a s_m$ rule:

$$s_{a_{eq_i}} = \frac{s_{a_i}}{[1 - (s_{m_i}/S_m)^s]^{1/r}} \quad \wedge \quad N_i = \frac{C}{(s_{a_{eq_i}})^B} \quad (7)$$

Despite its many shortcomings, most fatigue designers use the linear damage accumulation (or the Palmgren-Miner's) rule, $d = \sum d_i$, and predict failure (generation of a small crack in the SN method) when $\sum d_i = 1$, with $d = 1$ being the most used value. If this practice is sustained, it is quite easy to automate the SN method, combining the Wöhler, the $s_a s_m$, and the linear damage accumulation rules in just one equation:

$$d_i = \frac{n_i}{C} \left(\frac{s_{a_i}}{[1 - (s_{m_i}/S_m)^s]^{1/r}} \right)^B, \text{ if } s_{m_i} \geq 0, \text{ or} \quad (8a)$$

$$d_i = \frac{n_i}{C} \left(\frac{s_{a_i}}{[1 - (a \times s_{m_i}/S_m)]} \right)^B, \text{ if } s_{m_i} < 0 \quad (8b)$$

This equation can be implemented even in an Excel spreadsheet. But to increase the SN prediction accuracy and to remove one of the main Miner's rule shortcomings (and also to put some intellectual excitement in the SN, why not?), it is possible to modify the traditional SN methodology to consider plasticity induced loading sequence effects. The idea is simple (but not easy to be computationally implemented), and can be summarized as follows.

First, the initial residual stress state must be known at the critical point. Residual stresses act as mean loads, and must be added to each s_{m_i} component. The complex load must be counted by the sequential rain-flow method, from the first load event. Every load peak $s_{max_i} = s_{a_i} + s_{m_i} + s_{res}$ must be compared to the (cyclic) yield strength. If $s_{max_i} > S_Y$ there is yielding at the notch root, and the software should at that instant change from the SN to the sequential ϵN method, to calculate not only the damage but also the change in the residual stress state induced by that load event. The sequential ϵN method keeps track of the correct hysteresis loops at the notch root, as discussed below. Then the software can turn back to the SN method, bringing the new s_{res} value to continue the damage calculations as before. The main advantage of this hybrid method is computational efficiency, as the SN equations are much simpler to solve than the ϵN equations. This idea has been successfully implemented in the software.

THE FATIGUE DESIGN OF WELDED STRUCTURES

The fatigue design of welded structures is a particularly simple sub-group of the SN method. It differs from the procedures explained above because it is based on tests done in full scale structures, not in small specimens. Small speci-

mens are not appropriate due to the very high residual stresses normally present in a weld fillet (which are partially alleviated when the structure is cut to make such small specimens) and due to the geometric characteristics of the fillets (such as size and distribution of pores and inclusions).

The design methodology is normalized by welding organizations (such as the IIW - International Institute of Welding or the AWS - American Welding Society), and it is based on only two simple premises, which assume that the fatigue strength of a welded structural component (executed according to industrial quality control standards in C or C-Mn structural steel with $S_U \leq 700\text{MPa}$) just depends on [8]:

- the geometry or the type of the welding detail, which is classified in several classes by the different organizations (such as those in Figure 4, which presents some IIW details); and
- the range of the nominal load $\Delta\sigma$.

It should be noticed that this methodology has two significant differences in relation to the procedures used in the traditional SN method, because it does **not** depend on:

- the base material (from the fatigue point of view, it does not matter if S_U is 400 or 700MPa), and
- the applied mean load.

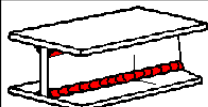
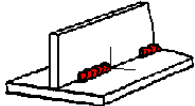
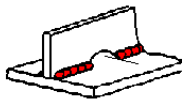
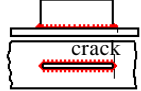
	Continuous manual longitudinal fillet or butt weld ($\Delta\sigma$ in flange adjacent to weld).	Class 100
	Intermittent longitudinal fillet weld ($\Delta\sigma$ in flange at weld ends).	80
	Longitudinal butt weld or fillet weld with cope holes ($\Delta\sigma$ in flange at weld ends).	71
	Longitudinal fillet gusset shorter than 150mm: longer than 150mm: near the edge:	71 63 50

Figure 4 – Some IIW welding details.

The several welding details are divided into classes of same fatigue strength, whose notation varies among the various organizations. The IIW classes varies between 45 and 125, and are denominated by the value of the stress range in MPa that the welding detail can support with a minimum fatigue life of $2 \cdot 10^6$ cycles, with a reliability of 97.7% (two standard deviations). Hence the fatigue strength of welded structures is quite low: the allowable $s_a = D s / 2$ varies from 5.6% to just 15.6% of the A36 steel ultimate strength ($S_U = 400\text{MPa}$). Each weld class is associated with an SN curve and a fatigue limit, defined at $5 \cdot 10^6$ cycles. Since the fatigue tests are made with full scale components, the

SN curves already include stress concentration, surface finish and residual stress effects.

Hence, it is easy to understand the strange, but physically reasonable, s_m independence hypothesis when fatigue designing welded structures: mean load effects are negligible because the mean load (the residual stress) is very high to start with. In fact, residual stresses in weld fillets frequently are tractive and higher than the yield strength. Since fatigue loads must be small, the s_{m_i} do not significantly change the effective mean load given by $s_{m_i} + s_{res}$ (Figure 5).

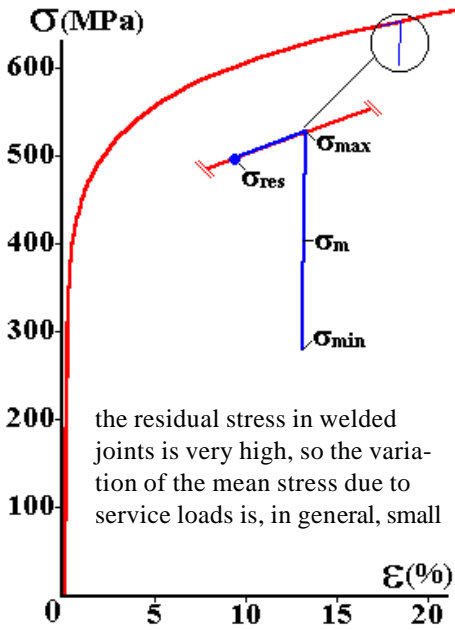


Figure 5 – The s_m variation in weld fillets is small because s_{res} is large

The automation of this methodology is a simple task. The fatigue strength of the welding detail is specified by its SN curve, given by $N D s^B = C$ (where $B = 3$ or 3.5 in the IIW procedures), and by its fatigue limit $D s_L$ (which in fact is the only independent information, and would have been a better choice to name the welding classes). The range of each load event $D s_i$ must be counted by the rain-flow method following the procedures already discussed in the SN method. Since the rain-flow counts $1/2$ cycles, the damage caused by a load sequence is given by:

$$d = \dot{a} d_i = \dot{a} \frac{D s_i^B}{2C} \quad (9)$$

The IIW fatigue design method has been implemented in the **V i D a** software, which also includes all databases required for its application.

THE eN METHOD

The eN method correlates the number of cycles N to initiate a fatigue crack in any structure with the life (in cycles) of small specimens that should (i) have the same fatigue strength (hence, the same material and details) and (ii) be submitted to the same *strain* history that loads the structure critical point (generally a notch root) in service. Therefore, the eN and the SN methods are based in similar philosophies. However, the eN recognizes macroscopic elastic-plastic events at the notch roots and uses the local strain range (a more robust parameter to describe plastic effects) instead of the stress range to quantify them. Therefore, the eN design routine is to:

- evaluate the critical point fatigue strength,
- calculate the critical point strain history, considering strain concentration effects, and
- quantify the damage accumulated by each load event.

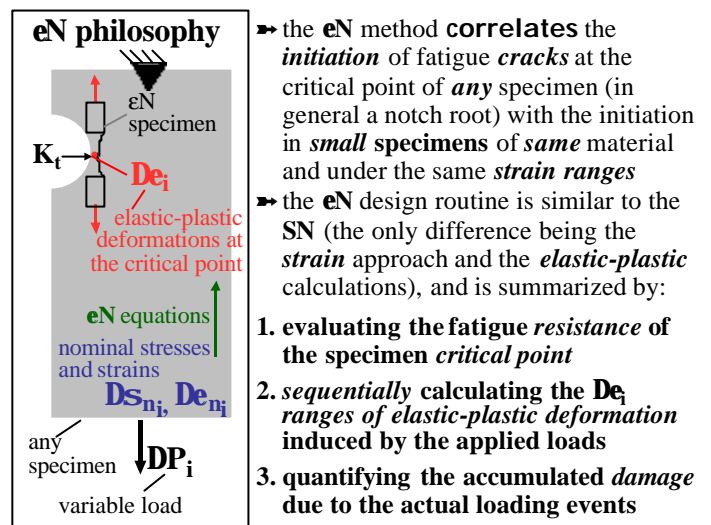


Figure 6 – The philosophy of the eN method.

Macroscopic plastic strain ranges cyclically move dislocations and can quickly induce fatigue cracks. Hence, the low-cycle fatigue strength is much less influenced by the critical point details such as surface roughness and strain gradients than the high-cycle, and it is controlled primarily by the material ductility. The eN method must be used to model low cycle problems, when the plastic strain range $D e_p$ at the critical point is of the same order or larger than the elastic range $D e_e$, but it can be applied to predict any initiation life. This model requires 4 pieces of information:

1. a $D s D e$ relationship, to describe the elastic-plastic hysteresis loops at the critical point;
2. a strain concentration rule, to correlate the nominal stress range $D s_n$ with the strain range $D e$ it induces at the critical notch root;
3. a $D e N$ relationship, to correlate the strain range $D e$ with the fatigue crack initiation life N ; and
4. a damage accumulation model.

The ϵN is a modern design method, corroborated by traditional institutions such as the SAE [9], but it has certain relatively little known idiosyncrasies. Particularly when dealing with complex loads, it is *not* possible to predict physically acceptable strain ranges at the critical point without recognizing the load *order*. Since plasticity generates memory, sequence effects must be accounted for when accurately modeling elastic-plastic hysteresis loops. In reality, precise fatigue life predictions require an accurate description of the stress-strain *history* at the critical point. In practice, such predictions can only be made with the aid of an appropriate automation software, since the numerical effort to sequentially solve the ϵN equations is quite heavy. Moreover, as the loop predictions are difficult, the software must have powerful graphical tools, to allow for the visual checking of the calculated hysteresis loops.

The classic ϵN method works with real (logarithmic) stresses and strains, uses a Ramberg-Osgood description for the $\Delta\sigma\Delta\epsilon$ loops, and considers the cyclic softening or hardening of the material, but not its transient behavior from the monotonic $\sigma\epsilon$ curve. Hence, a single equation is used in the ϵN method to describe all hysteresis loops:

$$e_a = \frac{D_e}{2} = \frac{D_{e_e}}{2} + \frac{D_{e_p}}{2} = \frac{D_s}{2E} + \frac{\alpha D_s \bar{\sigma}}{\epsilon 2H\epsilon_0}^{1/h\epsilon} \quad (10)$$

where E is the Young's modulus, H' is the hardening coefficient and h' is the hardening exponent of the cyclically stabilized $D_s D_e$ curve. Figures 7 and 8 [13] justify this simplification.

Neuber is the most used rule to correlate the nominal stress D_{s_n} and strain D_{e_n} ranges with the stress D_s and strain D_e ranges they induce at a notch root:

$$K_t^2 = \frac{D_s \times D_e}{D_{s_n} \times D_{e_n}} \quad (11)$$

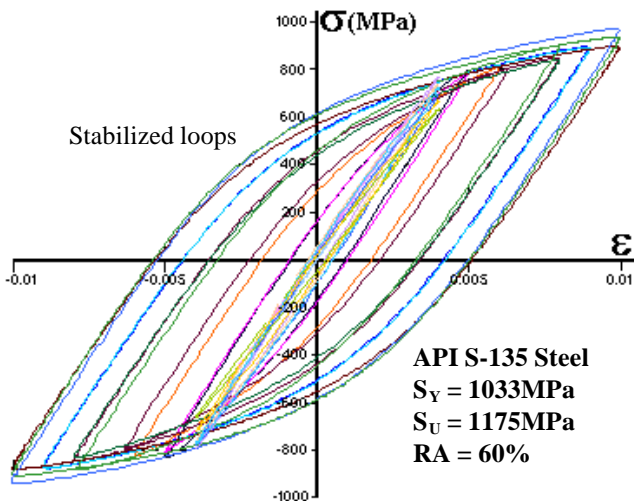


Figure 7 – Stabilized hysteresis loops measured in an API S-135 steel.

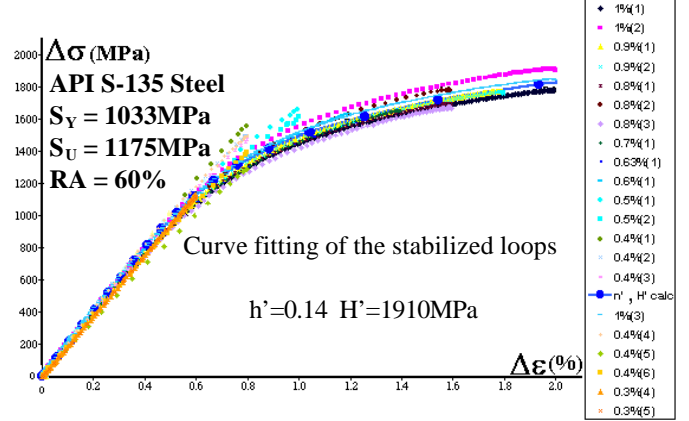


Figure 8 – Ramberg-Osgood fitting of the stabilized loops from Figure 7. All loops were moved to a common origin, and their unloading part was reflected over the positive.

When the nominal loads are elastic, it is common practice to use Neuber rule in the form:

$$K_t^2 = \frac{D_s \times D_e \times E}{D_{s_n}^2} \quad (12)$$

However, this practice is logically incongruent, since it treats the same material by two different models: Ramberg-Osgood at the notch root and Hooke at the nominal region, a procedure that can generate significant numerical errors when $D_{s_n}/2 > 0.7 \sim 0.8 S_Y$. In such cases (and to avoid offending the logical sense), it is worth using the Ramberg-Osgood model to describe the nominal loads too:

$$\frac{D_{e_n}}{2} = \frac{D_{s_n}}{2E} + \frac{\alpha D_{s_n} \bar{\sigma}}{\epsilon 2H\epsilon_0}^{1/h\epsilon} \quad (13)$$

Given D_{s_n} , it is operationally easier to first calculate D_s and then D_e from (10), (11) and (13):

$$K_t^2 \left(D_{s_n}^2 + \frac{2E D_{s_n}^{(h\epsilon+1)/h\epsilon}}{(2H\epsilon)^{1/h\epsilon}} \right) = D_s^2 + \frac{2E D_s^{(h\epsilon+1)/h\epsilon}}{(2H\epsilon)^{1/h\epsilon}} \quad (14)$$

$$D_e = \frac{D_s}{E} + 2 \frac{\alpha D_s \bar{\sigma}}{\epsilon 2H\epsilon_0}^{1/h\epsilon}$$

Given D_{s_n} , the material properties E , H' and h' , and the elastic stress concentration factor K_t , the notch root stress and strain ranges D_s and D_e are calculated by an appropriate numerical algorithm. The relationship between the critical point stress range D_e and its fatigue initiation life N is usually given by the classical Coffin-Manson rule:

$$\frac{D_e}{2} = \frac{s_f}{E} (2N)^b + e_f (2N)^c \quad (15)$$

where s_f , e_f , b and c are material constants, which are normally measured in fully alternated traction-compression

fatigue tests. The effect of a mean stress \mathbf{s}_m at the critical point is usually calculated by one of the three following rules:

$$\frac{\mathbf{D}e}{2} = \frac{\mathbf{s}_f - \mathbf{s}_m}{E} (2N)^b + e_f (2N)^c \quad (16)$$

$$\frac{\mathbf{D}e}{2} = \frac{\mathbf{s}_f - \mathbf{s}_m}{E} (2N)^b + e_f \frac{\mathbf{s}_f - \mathbf{s}_m}{\mathbf{s}_f} \frac{\bar{\sigma}_b}{\bar{\sigma}} (2N)^c \quad (17)$$

$$\frac{\mathbf{D}e}{2} = \frac{\mathbf{s}_f^2}{E \times \mathbf{s}_{\max}} (2N)^{2b} + \frac{\mathbf{s}_f \times e_f}{\mathbf{s}_{\max}} (2N)^{b+c} \quad (18)$$

Depending on the reference, (16) is called the Morrow and (17) the modified Morrow, or vice versa. To avoid this confusion (16) can be called the Morrow elastic and (17) the Morrow elastic-plastic equation, while (18) is known as the Smith-Topper-Watson equation.

There is vast experimental support to justify the use of these ϵN equations to predict fatigue crack initiation under simple loads. However, when using this method under complex loading, it is common to neglect loading order effects and to simply calculate the damage caused by the i -th load event as if it was independent of all others. Hence, the idea is to rain-flow count the nominal loads $\mathbf{D}\mathbf{s}_{ni}$, use Equation (14) to calculate the corresponding $\mathbf{D}e_i$ and Equation (15) to predict N_i and the damage \mathbf{d}_i (which by the linear law is $\mathbf{d}_i = 1/2N_i$, where N_i has already been defined in the SN method).

Given the i -th nominal load event $\mathbf{D}\mathbf{s}_{ni}$, the notch root strain range $\mathbf{D}\mathbf{s}_i$ is calculated by:

$$(\mathbf{K}_t \mathbf{D}\mathbf{s}_{ni})^2 = \mathbf{D}\mathbf{s}_i \times \frac{\mathbf{s}_f}{E} \mathbf{D}\mathbf{s}_i + 2E \times \frac{\mathbf{s}_f}{E} \frac{\bar{\sigma}_b}{\bar{\sigma}} \frac{1}{2H} \frac{\bar{\sigma}_b}{\bar{\sigma}} \quad (19)$$

The corresponding strain range $\mathbf{D}e_i$ and damage \mathbf{d}_i are then calculated by:

$$\frac{\mathbf{D}\mathbf{s}_i}{E} + 2 \times \left(\frac{\mathbf{D}\mathbf{s}_i}{2H} \right)^{\frac{1}{H}} = \mathbf{D}e_i = \frac{2\mathbf{s}_f}{E} (2N_i)^b + 2e_f (2N_i)^c$$

$$\mathbf{D} \mathbf{d}_i = \frac{n_i}{2N_i} \quad (20)$$

These equations can not be inverted, hence the use of the ϵN method is computationally difficult, explaining (but not justifying) the indiscriminate use of these equations, since

The application of these equations to the rain-flow count of the nominal loads usually does not generate predictions of physically acceptable hysteresis loops!

In fact, to guarantee the quality of the predictions it is indispensable to first assure that the calculation model reproduces the hysteresis loops at the critical point, for only then calculating the damage caused by the loops. Even if the piece is virgin, if the residual stress and strain state is zero, and if the cyclical hardening or softening transient can be neglected, the increments of plastic strain are dependent on the load history and it is necessary to distinguish the first 1/2 cycle from the subsequent load events. Even in the idealized case, the first 1/2 cycle departs from the origin of the $\sigma\epsilon$ plane following the (cyclic) $\sigma\epsilon$ curve and not the loop equation:

$$(\mathbf{K}_t \mathbf{s}_{n0})^2 = \mathbf{s}_0 \times \frac{\mathbf{s}_f}{E} \mathbf{s}_0 + E \times \frac{\mathbf{s}_f}{E} \frac{\bar{\sigma}_b}{\bar{\sigma}} \frac{1}{2H} \frac{\bar{\sigma}_b}{\bar{\sigma}} \quad (21)$$

$$\frac{\mathbf{s}_0}{E} + \frac{\mathbf{s}_f}{E} \frac{\bar{\sigma}_b}{\bar{\sigma}} \frac{1}{2H} \frac{\bar{\sigma}_b}{\bar{\sigma}} = e_0 = \frac{2\mathbf{s}_f}{E} (2N_0)^b + 2e_f (2N_0)^c$$

$$\mathbf{D} \mathbf{d}_0 = \frac{1}{2N_0} \quad (22)$$

But this indispensable care is still not enough. As illustrated in Figure 9, it is also necessary to guarantee that all the subsequent events do not surpass (i) the cyclic $\sigma\epsilon$ curve, nor (ii) the wrapper of the hysteresis loops. Hence, the automation software should verify if and when the predicted strains (by the equation of the hysteresis loop applied for each load event $\mathbf{D}\mathbf{s}_i, \mathbf{D}e_i$) cross the cyclic $\sigma\epsilon$ curve or a previously induced loop. At the crossing point, the software must change the equation of that i -th event, and it must follow the cyclic $\sigma\epsilon$ curve or the curve of the previously induced loop until the end of that i -th load event.

The computational details of this complicated calculation step are considered beyond the scope of this paper, but are discussed elsewhere [14]. However, it is worth emphasizing these corrections are indispensable under penalty of generating predictions that are (i) physically inadmissible, and (ii) probably *not* conservative. As shown in Figure 9, only after applying all the required corrections it is possible to predict decent loops and, hence, the correct fatigue damage if the load is complex.

To guarantee the precision of the calculations, the **V i D a** software includes the corrections discussed above, besides a series of other equally important features such as:

- it draws the ϵN curve and plots over it the traditional SN curve for comparison purposes, and it can force the elastic component of the ϵN curve to reach \mathbf{S}_L at the specified fatigue limit life;
- it allows the Neuber rule to be changed by the linear strain concentration rule;

- it calculates and draws the properly corrected hysteresis loops, but it can also calculate them by the non-sequential ϵN method;
- for comparison purposes, it calculates fatigue life by five methods: Coffin-Manson and Manson's universal slopes, which do not consider the mean load effects, and by Morrow elastic, Morrow elastic-plastic and Smith-Topper-Watson, calculating s_m at the critical point considering all the loop corrections;
- it generates graphs of damage versus event for each one of the calculation models.

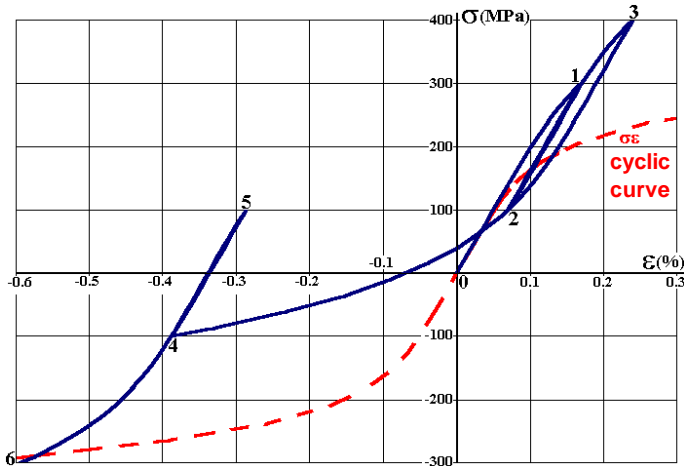


Figure 9a – Uncorrected loops predicted for the load $\{0 \rightarrow 300 \rightarrow 100 \rightarrow 400 \rightarrow 100 \rightarrow 100 \rightarrow 300\}$ MPa applied upon a smooth ϵN specimen of an SAE1020 steel [12], with $E=203\text{GPa}$, $H'=772\text{MPa}$, $h'=0.18$, $S_f=896\text{MPa}$, $e_f=0.41$, $b = -0.12$ and $c = -0.51$, *without* considering sequence effects. Calculated damage: $d = 2.9 \times 10^{-5}$.

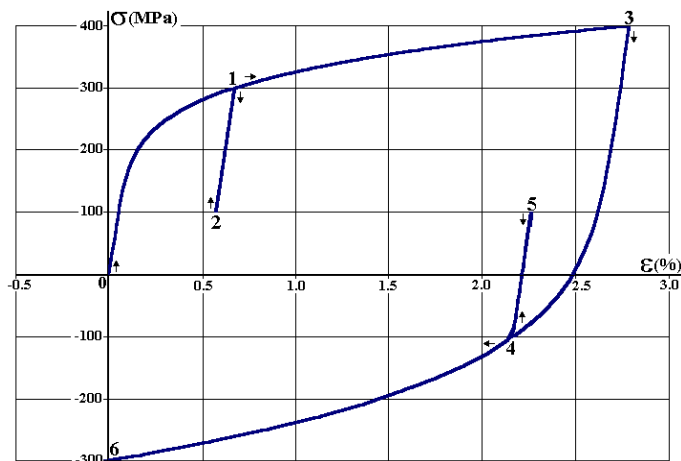


Figure 9b – Loops predicted for the problem in Figure 9a, *considering* the proposed corrections. Calculated damage: $d = 1.3 \times 10^{-3}$.

To illustrate the accuracy of these predictions, Figure 10 compares predicted and experimental loops measured in API S-135 steel under complex load.

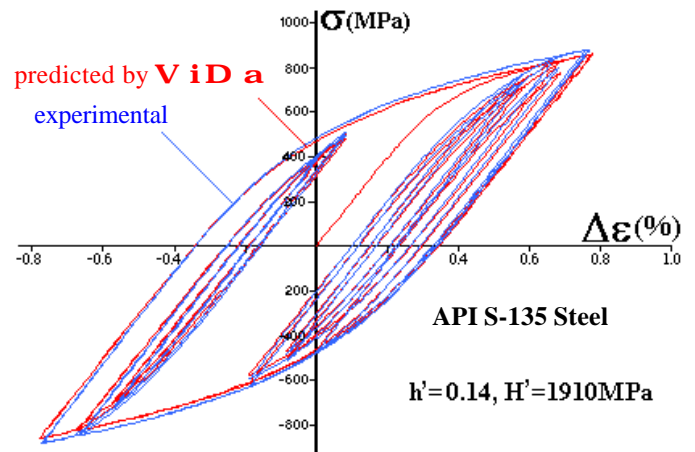


Figure 10 – Predicted and experimentally measured loops [13].

THE da/dN METHOD

The modeling and the reckoning automation by the **local** approach of the LEFM mode I fatigue crack propagation under complex loading are discussed below. The loading, whose amplitude can randomly vary in time, has unlimited complexity. Sequence effects, such as overload-induced crack retardation or arrest are also considered. Only mode I [17-20] is discussed, since fatigue cracks almost always propagate perpendicular to the maximum tensile stress.

The local approach is so called because it does not require the global solution of the structure's stress field, since it is based on the direct integration of the fatigue crack propagation rule of the material, $da/dN = F(DK, R, DK_{th}, K_C, \dots)$, where DK is the stress intensity range, $R = K_{min}/K_{max}$ is a measure of the mean load, DK_{th} is the fatigue crack propagation threshold and K_C is the structure toughness. An appropriate stress intensity factor expression for DK and a good da/dN rule must be used to obtain satisfactory predictions. Therefore, neither the DK expression nor the type of crack propagation rule should have their accuracy compromised when using this approach.

The following topics are discussed: (i) the DK_{rms} method, including the differences between 1D and 2D crack propagation modeling; (ii) the cycle-by-cycle method; (iii) some proposals for increasing the computational efficiency of the models; and (iv) the modeling of load sequence effects. Finally, the advantages and limitations of the several studied models are evaluated.

THE ΔK_{rms} METHOD – The stress intensity factor range is expressed as $DK = Ds \times [\bar{\sigma}(pa) \times f(a/W)]$, where Ds is the nominal stress range (in relation to which the DK expression is defined), a is the crack length, $f(a/W)$ is a non-dimensional function of a/W , and W is a characteristic dimension of the structure. Therefore, Ds quantifies the influence of the loading and $\bar{\sigma}(pa) \times f(a/W)$ quantifies the ef-

fect of the geometry of the piece and of the crack shape and size in \mathbf{DK} .

The simplest way to treat the fatigue life prediction under complex loading problem is to substitute it by a simple equivalent loading, causing the same crack growth. It has been experimentally discovered that \mathbf{DK}_{rms} , the root mean square value of the stress intensity range, can in many cases be used for this purpose [15].

According to Hudson [16], \mathbf{DK}_{rms} can be calculated from the **rms** values of the positive peaks and valleys of the loading (since the crack does not grow while closed, the compressive part of the loading is discarded). Therefore:

$$s_{\text{max}_{\text{rms}}} = \sqrt{\frac{\sum_{i=1}^p \dot{a}(s_{\text{max}_i})^2}{p}}, \quad (s_{\text{max}_i} \geq 0) \quad (23)$$

$$s_{\text{min}_{\text{rms}}} = \sqrt{\frac{\sum_{i=1}^q \dot{a}(s_{\text{min}_i})^2}{q}}, \quad (s_{\text{min}_i} \leq 0) \quad (24)$$

$$\mathbf{DS}_{\text{rms}} = s_{\text{max}_{\text{rms}}} - s_{\text{min}_{\text{rms}}} \quad \text{and} \quad \mathbf{R}_{\text{rms}} = \frac{s_{\text{min}_{\text{rms}}}}{s_{\text{max}_{\text{rms}}}} \quad (25)$$

As $\mathbf{DK}_{\text{rms}} = \mathbf{DS}_{\text{rms}} \times [\mathbf{0}(\mathbf{pa}) \times \mathbf{f}(a/W)]$, the number of cycles the crack takes to grow from the initial length \mathbf{a}_0 to the final one \mathbf{a}_f is given by:

$$N = \int_{\mathbf{a}_0}^{\mathbf{a}_f} \frac{da}{\mathbf{0}_{\mathbf{F}(\mathbf{DK}_{\text{rms}}, \mathbf{R}_{\text{rms}}, \mathbf{DK}_{\text{th}}, \mathbf{K}_c, \dots)}} \quad (26)$$

In the **V i D a** software, a variation of the Simpson's algorithm can be used for numerical integration of the simple loading case and, consequently, also for the \mathbf{DK}_{rms} method. Crack increments $\mathbf{da} > 0.1 \text{ mm}$ for the discretization of the integral can be specified by the user, who can also choose an integration method based on adjustable steps depending on the variation of the crack length, as it will be discussed later on the cycle-by-cycle method.

The \mathbf{DK}_{rms} value of a complex loading is similar but not identical to the \mathbf{DK} of a simple loading. As any statistics, \mathbf{DK}_{rms} does not recognize temporal order, and cannot detect some important problems such as:

- Sudden fracture caused by a single large peak during the complex loading (to start the fracture process, it is enough that in just *one* event $\mathbf{K}_{\text{max}} \geq \mathbf{K}_c$).
- Any interaction among the loading cycles (e.g., crack retardation or arrest phenomena after an overload).

- It is *not* possible to guarantee the inactivity of the crack if $\mathbf{DK}_{\text{rms}}(\mathbf{a}_0) < \mathbf{DK}_{\text{th}}(\mathbf{R}_{\text{rms}})$.

In complex loading, this latter threshold problem can be caused by all the $(\mathbf{DS}_i, \mathbf{R}_i)$ events that induce $\mathbf{DK}_i > \mathbf{DK}_{\text{th}}(\mathbf{R}_i)$, which can make the crack grow even if $\mathbf{DK}_{\text{rms}} < \mathbf{DK}_{\text{th}}(\mathbf{R}_{\text{rms}})$. Therefore, as \mathbf{DK}_i depends both on the stress range \mathbf{DS}_i and on the crack size \mathbf{a}_i in that event, even if the value of \mathbf{DS}_{rms} stays constant, the same cannot be guaranteed for \mathbf{DK}_{rms} .

Equation (26) can only be applied to 1D cracks, but in practice many times it is necessary to study surface, corner or internal cracks, which spread in 2D. The principal characteristic of these cracks is a non-homologous fatigue propagation: in general, the crack shape tends to change from cycle to cycle, because \mathbf{DK} varies from point to point along the crack front. This problem is beyond the scope of this paper, but has been recently discussed in [2].

THE CYCLE-BY-CYCLE METHOD – The basic idea of this method is to associate to each load reversion the growth that the crack would have if that 1/2 cycle was the only one to load the piece (this implies in neglecting interaction effects among the several events of a complex loading, such as overload-induced retardation or stop in the crack growth). Using this assumption, it is easy to write a general expression for the cycle-by-cycle crack growth, using any crack propagation rule: if $da/dN = \mathbf{F}(\mathbf{DK}, \mathbf{R}, \mathbf{DK}_{\text{th}}, \mathbf{K}_c, \dots)$, and if in the i -th 1/2 loading cycle the length of the crack is \mathbf{a}_i , the stress range is \mathbf{DS}_i and the mean load causes \mathbf{R}_i , then the crack grows by a \mathbf{da}_i given by:

$$\mathbf{da}_i = \frac{1}{2} \times \mathbf{F}(\mathbf{DK}(\mathbf{DS}_i, \mathbf{a}_i), \mathbf{R}(\mathbf{DS}_i, \mathbf{s}_{\text{max}_i}), \mathbf{DK}_{\text{th}}, \mathbf{K}_c, \dots) \quad (27)$$

The total growth of the crack is quantified by $\mathbf{S}(\mathbf{da}_i)$. Therefore, the cycle-by-cycle rule is similar in concept to the linear damage accumulation used in the SN and ϵN fatigue design methods. And, as in Miner's rule, it requires that *all* the events that cause fatigue damage be recognized before the calculation, by rain-flow counting the loading. However, this counting algorithm alters the *order* of the loading, as shown in Figure 3. This can cause serious problems in the predictions, because the loading order effects in crack propagation are of two different natures:

- Delayed effects, that can retard or stop the subsequent growth of the crack due, e.g., to plasticity-induced Elber-type crack closure [31] or to crack tip bifurcation. These interaction effects among the loading cycles normally increase the crack life and, if neglected in the cycle-by-cycle calculation, may induce excessively conservative predictions.

- Instantaneous fracture, that occurs when $K_{max} \geq K_C$ in *one* event, which must be precisely predicted.

As already mentioned above, the loading input in the **VIDA** software is sequential, and preserves the time order information that is lost when histograms or any other loading statistics are generated. To take advantage of this feature, a *sequential* rain-flow counting option has been introduced in that software. With this technique, the effect of each large loading event is counted when it happens (and not before its occurrence, as in the traditional rain-flow method). The main advantage of the sequential rain-flow counting algorithm is to avoid the premature calculation of the overload effects, which can cause *non-conservative* crack propagation life predictions (as $K(s, a)$ in general grows with the crack, a given overload applied when the crack is large can be much more harmful than applied when the crack is small). The sequential rain-flow does not eliminate all the sequencing problems caused by the traditional method, but it is certainly an advisable option because it presents advantages over the original algorithm, without increasing its complexity.

As discussed in the DK_{rms} method, the compressive part of the loading can be discarded in the calculations, that is, the negative peaks and valleys can be zeroed before the computations to decrease the numerical effort of the cycle-by-cycle method. And, in the same way, a range filtering option can be very useful to discard the small loads that cause no damage inducing $DK_i < DK_{th}(R_i)$.

The range filtering can indeed significantly reduce the computational effort in fatigue damage calculations if the complex loading history is long. But this procedure is intrinsically *non-conservative*, since it can disregard damaging events, because DK_i is not available before the crack growth calculations (DK depends not only on the loads, but also on the crack size). The conservative rule is to limit the cut of the loading to the pairs (Ds_i, R_i) that cause $DK(a_f) < DK_{th}[R(a_f)]$, where a_f is the expected final length for the crack. But, in practice, it is easier to numerically try decreasing the ranges for the filtering, until there is no significant variation in the results.

The computational implementation of equation (27), even with the pre-zeroing of the compressive peaks and valleys and with the range filtering of the loading, is still not numerically efficient. For this reason, an additional feature to reduce the computational time is quite useful: the option of maintaining the geometrical part of DK constant during small variations in crack size. As $DK = Ds_i \times [\bar{O}(pa_i) \times f(a_i/W)]$, where $f(a/W)$ is a non-dimensional function (usually complicated) that depends only on the piece and crack geometry and not on the loading, it can be said that the range of the

stress intensity factor DK_i at each load reversion depends on two variables of different nature:

- on the stress range Ds_i in that event, and
- on the length of the crack a_i in that instant.

Ds_i , of course, can vary significantly at each load reversion when the loading is complex, but fatigue cracks always grow very slowly. In fact, at least in structural metals, the largest rates of stable crack growth observed in practice are of the order of $\mu\text{m}/\text{cycle}$, and during most of the life the crack growth rates are better measured in nm/cycle .

However, as in general the usually complicated $f(a/W)$ expressions do not present discontinuities, one can take advantage of the small changes in $f(a/W)$ during small increments in crack length. In this way, instead of calculating at each load cycle the value of $DK_i = Ds_i \times [\bar{O}(pa_i) \times f(a_i/W)]$, a task that demands great computational effort, it is more efficient to hold $f(a_i/W)$ constant during a (small) percentage of crack increment $da\%$, that should be specifiable by the calculation software user.

The errors introduced by this procedure are non-conservative, but they decrease quickly with the specified value for $da\%$. And, as in the range filtering case, it is easier to begin with a higher value to minimize the computational time, and to numerically try to find the most convenient $da\%$ value to the problem in hand.

LOAD CYCLE INTERACTION EFFECTS – It is a well known fact that interaction problems among load cycles can have a very significant effect on the prediction of fatigue crack growth. There is a vast literature proving that tensile overloads, when applied over a loading whose amplitude otherwise stays constant, can cause retardation or arrest in the crack growth (see, e.g., Figure 11), and that even compressive overloads can sometimes affect the rate of subsequent crack propagation [11,12,17-19].

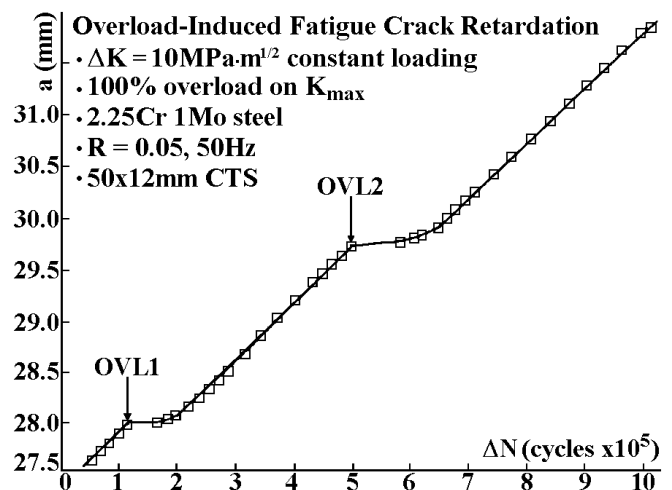


Figure 11 – Fatigue crack growth retardation induced by tensile overloads.

Neglecting these effects in fatigue life calculations can completely invalidate the predictions. In fact, only after considering overload induced retardation effects can the life reached by real structural components be justified when modeling many practical problems. However, the generation of an universal algorithm to quantify these effects is particularly difficult, due to the number and to the complexity of the mechanisms involved in fatigue crack retardation, among them:

- plasticity-induced crack closure,
- blunting and/or bifurcation of the crack tip,
- residual stresses and/or strains,
- strain-hardening,
- crack face roughness,
- oxidation of the crack faces.

Besides, depending on the case, several of these mechanisms may act concomitantly or competitively, as a function of factors such as:

- crack size,
- microstructure of the material,
- dominant stress state, and
- environment.

The detailed discussion of this complex phenomenology is considered beyond the scope of this work (a revision of the phenomenological problem can be found in [11]). Moreover, the relative importance of the several mechanisms can vary from case to case, and there is so far no universally accepted single equation capable of describing the whole problem. Therefore, from the designer's point of view, it must necessarily be treated in the most reasonably simplified way.

But a simplified model must not be unrealistic, and so it is worthwhile mentioning that some simplistic models are unacceptable. For instance, it is not reasonable to justify the retardation effects by attributing to the overloads a significant variation in the residual stress state *at* the crack tip. This is mechanically impossible: the tensile yielding during the loading and the compressive yielding during the unloading close to the crack tip during fatigue crack propagation prevent any significant variation in the residual stress state *at* the crack tip after an overload. On the other hand, the principal characteristic of fatigue cracks is to propagate cutting a material that has already been deformed by the plastic zone that always accompanies their tips. The fatigue crack faces are embedded in an envelope of (plastic) residual strains and, consequently they:

- compress their faces when completely discharged, and
- open alleviating in a progressive way the (compressive) load transmitted through their faces.

According to Elber [21], only after completely opening the crack at a load K_{op} , would the crack tip be stressed.

Therefore, the bigger the K_{op} , the less would be the effective stress intensity range $DK_{ef} = K_{max} - K_{op}$, and this DK_{ef} instead of DK would be the crack propagation rate controlling parameter. Most load interaction models are, although indirectly, based in this idea. This implicates in the supposition that the main retardation mechanism is caused by plasticity induced crack closure: in these cases, the opening load should *increase* when the crack penetrates into the plastic zone inflated by the overload, *reducing* the DK_{ef} and stopping or delaying the crack, while the plastic zones associated with the loading are contained in the overload induced plastic zone.

But it is very important to emphasize that this is by no means the only mechanism that can induce crack retardation. For example, Castro & Parks [22] showed that, under dominant plane strain conditions, overload induced fatigue crack retardation or stop can occur while DK_{ef} *increases* (Figure 12). The principal retardation mechanism in those cases was bifurcation of the crack tip.

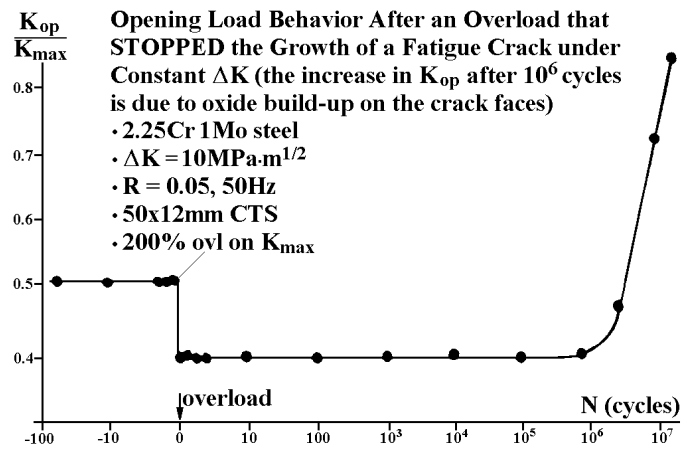


Figure 12 – Opening load versus number of cycles after an overload that *stopped* the fatigue crack growth. Just after the overload the opening load *decreased*, a behavior completely incompatible with Elber-type crack closure.

Wheeler is the most popular retardation model [18,23]. The model is simplistic and assumes, more or less arbitrarily, that while the loading plastic zone ZP_i is embedded in the overload plastic zone ZP_{ov} , the crack growth rate retardation depends on the distance from the border of ZP_{ov} to the tip of the crack, see Figure 13.

In the Wheeler model, the retardation is maximum just after the overload, and stops when the border of ZP_i touches the border of ZP_{ov} . Therefore, if a_{ov} and a_i are the crack sizes at the instant of the overload and at the *i*-th cycle, and $(da/dN)_{ret_i}$ and $(da/dN)_i$ are the retarded and the non-retarded crack growth rates (at which the crack would be

growing in the i -th cycle if the overload had not occurred), then, according to Wheeler:

$$\frac{da}{dN}_{ret} = \frac{da}{dN} \times \frac{ZP_i}{a_{ov} + ZP_{ov} - a_i}^b, a_i + ZP_i < a_{ov} + ZP_{ov} \quad (28)$$

where b is an experimentally adjustable constant. Broek [33, 34] mentions Wheeler's data for steels ($b = 1.43$) and for Ti-6AL-4V ($b = 3.4$), and suggests that other typical values for b are between 0 and 2.

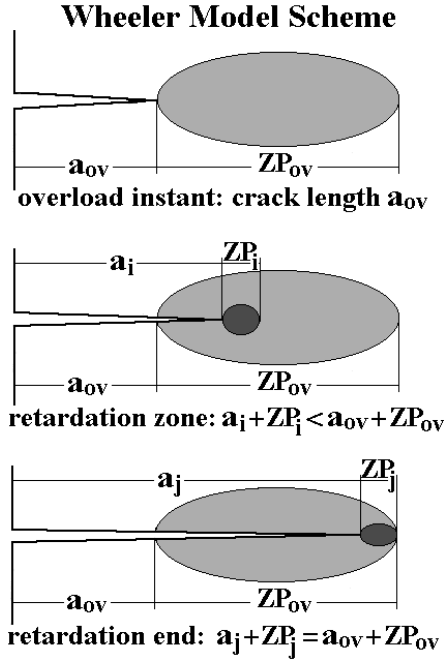


Figure 13 – Wheeler crack growth retardation model.

It should be noticed that this model cannot predict the observed crack stops. As $ZP \gg (K_{max}/S_Y)^2$, where S_Y is the yielding strength of the material, the maximum value of the predicted retardation happens immediately after the overload, and is equal to $(K_{max}/K_{ov})^{2b}$, where K_{max} is the maximum load in the cycle just after the overload, and K_{ov} is the overload peak. Therefore, the phenomenology of the load cycle interaction problem is not completely reproducible by the Wheeler original model. However, to also model crack stops, a simple modification that seems reasonable is to use a Wheeler-like parameter to multiply DK instead of da/dN after the overload [12]:

$$DK_{ret}(a_i) = DK(a_i) \times \frac{ZP_i}{a_{ov} + ZP_{ov} - a_i}^g, a_i + ZP_i < a_{ov} + ZP_{ov} \quad (29)$$

where $DK_{ret}(a_i)$ and $DK(a_i)$ are the values of the stress intensity factors that would be acting at a_i with and without retardation due to the overload, and g is in general different from the original model exponent b . This simple modification can be used with any of the propagation rules that recognize DK_{th} to predict both the retardation and the stop of fatigue cracks after an overload (the stop occurring if $DK_{ret}(a_i) < DK_{th}$).

The numerical implementation of these retardation models in a cycle-by-cycle algorithm is not conceptually difficult, but it requires a considerable programming effort. To illustrate the main ideas, a simplified flow-chart of the **ViDa** fatigue crack growth calculation algorithm is shown in Figure 14.

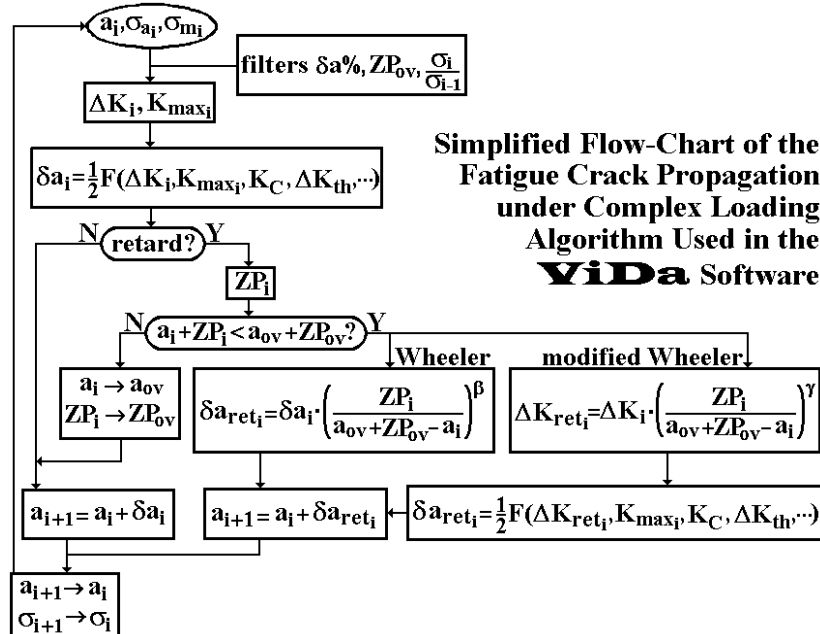


Figure 14 – Simplified flow-chart of the calculation algorithm used in the **ViDa** software to predict fatigue crack propagation under complex loading.

Some calculation details are worth mentioning. The first one refers to the use of the $\mathbf{da}\%$ filter, since crack size increments that work well otherwise can cause troubles with the retardation models, as the plastic zone sizes can be very small compared to the crack size. In order to quantify the propagation gradient inside the overload affected zone, $\mathbf{da}\%$ must be much smaller than \mathbf{ZP}_{ov} .

A second detail can save a lot of computational time when the loading is complex. Small variations in the loading amplitude do not cause experimentally detectable crack retardation, and they should not be considered as overloads in the calculation model. Therefore, a numerical filter for overloads can be profitably introduced in the algorithm, specifying that there is no overload effect if $\mathbf{s}_j/\mathbf{s}_{j-1} < \mathbf{a}$, where \mathbf{s}_{j-1} and \mathbf{s}_j are successive peaks of the loading and \mathbf{a} is an adjustable constant (that, in the absence of better information, can be chosen as 1.25 or 1.3).

Finally, it is worthwhile to remind that the border of the plastic zone moves forward with the crack. Therefore, in the complex loading case, the controlling border of the retardation zone advances as new overloads induce plastic zones that cross the previous frontier.

There are several other retardation models [11, 23], but none of those that can be implemented in a local approach code has definitive advantages over the simpler Wheeler models discussed above. This is no surprise, since single equations are too simplistic to model all the several mechanisms that can induce retardation effects. Therefore, in the same way that a curve $\mathbf{da}/d\mathbf{N}$ vs. \mathbf{DK} is experimentally measured, a propagation model can be adjusted to experimental data to calibrate the exponents of equations (28) or (29), as recommended by Broek [18].

FINITE ELEMENT CRACK PROPAGATION SIMULATION

A companion software, called **QUEBRA2D** (meaning 2D fracture in Portuguese) [2], has been developed as an interactive graphical software for simulating two-dimensional fracture processes based on a finite element adaptive mesh generation strategy. The adaptive process first requires the results from the analysis of an initial finite element mesh, usually rough, with the geometric descriptions, the boundary conditions, and their attributes. Then a discretization of the domain's region boundary is performed based on the geometric properties and on the characteristic sizes of the boundary elements (adjacent to the boundary curves), determined from the error estimate from the previous step of the finite element analysis.

An advantage of this strategy is that the boundary curve is discretized independently of the model's domain,

thus resulting in a more regular boundary discretization. From this discretization, the new mesh is generated, based on quadtree and Delaunay triangulation techniques. The quadtree generates the mesh in the interior of the model, leaving a band near the boundary to be discretized by the Delaunay triangulation. This process is repeated until the estimate discretization error reaches a predefined value.

Some other **QUEBRA2D** highlights are:

- Visualization of iso-strips and iso-lines from scalar results at the nodes and at the Gauss points.
- Stress-intensity factor computation by means of three methods:
 - Displacement Correlation Technique
 - Modified Crack Closure Method
 - J-intergral formulation with Equivalent Domain Integral Method
- Crack propagation direction computation by means of the following theories:
 - Maximum Circumferential Stress (\mathbf{S}_{qmax})
 - Maximum Potential Energy Release Rate (\mathbf{G}_{qmax})
 - Minimum Strain Energy Density (\mathbf{S}_{qmin})
- Vectorial plotting for visualizing the principal stress results.
- Visualization of the model's deformed configuration.
- Scalar result graphs along a section line in the model.
- Graphs for analyzing fatigue problems, with the possibility of selecting among several models for anticipating the structure's life under simple loading.
- History graphs with the stress-intensity factors for Modes I and II.
- Result of the integral of the curves generated in the graphs.
- Zoom, distortion, and translation specification.
- Visualization of node and element attributes.
- Visualization of the model's animation along the several steps.
- Option of the interface language.

The software has been implemented in C language, using the IUP/LUA interface system and the CD graphic system. This environment allows, without any code modification, automatic portability to several platforms, including workstations based on the Unix operational system and PCs running under Windows 98/2000 or NT.

CONCLUSIONS

This paper studied the fatigue design automation problem. Since fatigue crack generation depends primarily on the range of the *local* stress or strain acting on the critical point of the structure, and cracks larger than a few grain sizes have their fatigue propagation rate controlled primarily by the mode I stress intensity range, the fatigue design problem can in many cases be treated by local methods. A gen-

eral purpose fatigue design software was briefly presented. This software has been developed to predict both initiation and propagation fatigue lives under complex loading by all classical design methods: **SN**, **IIW** (for welded structures) and **eN** to predict crack initiation, and **da/dN** for studying plane and 2D crack propagation, *considering* load sequence effects. In particular, its crack propagation module accepts any stress intensity factor expressions, including the ones generated by a companion specialized finite-element software. Both software have been numerically and experimentally tested, and incorporate all the requirements that design automation tools must have.

REFERENCES

- [1] Meggiolaro, M.A. and Castro, J.T.P., “**V i d a 9 8** – a Visual Damagemeter to Automatize the Fatigue Design under Complex Loading,” (in Portuguese), *Revista Brasileira de Ciências Mecânicas*, v. 20, pp. 666-685, 1998.
- [2] Miranda, A.C.O., Meggiolaro, M.A., Castro, J.T.P., Martha, L.F., and Bittencourt, T.N. “Fatigue Crack Propagation under Complex Loading in Arbitrary 2D Geometries”, to be published in *Applications of Automation Technology in Fatigue and Fracture Testing and Analysis*, *ASTM STP 1411*, 2000
- [3] Bannantine, J.A., Comer, J.J. and Handrock, J.L. “Fundamentals of Metal Fatigue Analysis”, Prentice Hall 1990.
- [4] Dowling, N.E. “Mechanical Behavior of Materials”, Prentice-Hall 1993.
- [5] Fuchs, H.O. and Stephens, R.I. “Metal Fatigue in Engineering”, Wiley 1980.
- [6] Hertzberg, R.W. “Deformation and Fracture Mechanics of Engineering Materials”, Wiley 1989.
- [7] Juvinall, R.C. “Stress, Strain and Strength”, McGraw-Hill 1967.
- [8] Branco, C.M, Fernandes, A.A., and Castro, P.M.S.T. “Fadiga de Estruturas Soldadas”, Gulbenkian 1987.
- [9] Rice, R.C., ed. “Fatigue Design Handbook”, SAE 1988.
- [10] Shigley, J.E. and Mischke, C.R. “Mechanical Engineering Design”, McGraw-Hill 1989.
- [11] Suresh, S. “Fatigue of Materials”, Cambridge 1991.
- [12] Castro, J.T.P. and Meggiolaro, M.A. “Projeto à Fadiga sob Cargas Complexas”, in CD, 2000.
- [13] Guizzo, T. “Laços de Histerese Elastoplásticos Gerados sob Carregamentos Complexos”, MSc Thesis, Mech. Eng. Dept. PUC-Rio, 1999.
- [14] Castro, J.T.P. and Meggiolaro, M.A., “Some Comments on the eN Method Automation for Fatigue Dimensioning under Complex Loading,” (in Portuguese), *Revista Brasileira de Ciências Mecânicas*, v. 21, pp.294-312, 1999.
- [15] Barsom, J.M. and Rolfe, S.T., “Fracture and Fatigue Control in Structures”, Prentice-Hall, New Jersey, 1987.
- [16] Hudson, C.M., “A Root-Mean-Square Approach for Predicting Fatigue Crack Growth under Random Loading,” *ASTM STP 748*, pp.41-52, 1981.
- [17] Anderson, T.L. “Fracture Mechanics”, CRC, 1995.
- [18] Broek, D., “The Practical Use of Fracture Mechanics”, Kluwer 1988.
- [19] Broek, D., “Elementary Engineering Fracture Mechanics”, 4th ed., Martinus Nijhoff 1986.
- [20] Tada, H.; Paris, P.C. and Irwin, G.R. “The Stress Analysis of Cracks Handbook”, 1985.
- [21] Elber, W. “The Significance of Fatigue Crack Closure,” *ASTM STP 486*, 1971.
- [22] Castro, J.T.P. and Parks, D.M., “Decrease in Closure and Delay of Fatigue Crack Growth in Plane Strain,” *Scripta Metallurgica*, v.16, 1982, pp.1443-1445.
- [23] Chang, J.B and Hudson, C.M. ed., *Methods and Models for Predicting Fatigue Crack Growth Under Random Loading*, *ASTM STP 748*, ASTM, 1981.